Title

DICHOTOMOUS VIRTUAL IMPACTORS FOR LARGE SCALE MONITORING OF AIRBORNE PARTICULATE MATTER

Author

Loo, Billy W.

Publication Date

1975-05-01

Presented at the Symposium on Fine Particles, Minneapolis, MN, May 28 - 30, 1975

LBL-3854

DICHOTOMOUS VIRTUAL IMPACTORS FOR LARGE SCALE MONITORING OF AIRBORNE PARTICULATE MATTER

Billy W. Loo, Joseph M. Jaklevic, and Fred S. Goulding

May 1975

Prepared for the U. S. Energy Research and Development Administration under Contract W-7405-ENG-48

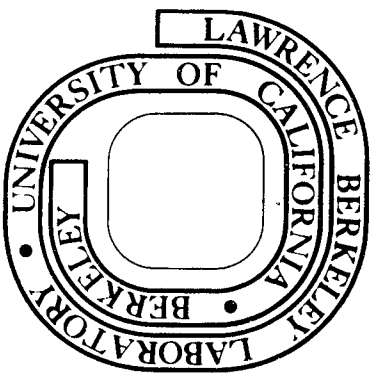

DISCLAIMER

DICHOTOMOUS VIRTUAL IMPACTORS FOR LARGE SCALE MONITORING OF AIRBORNE PARTICULATE MATTER *

Billy W. Loo, Joseph M. Jaklevic, and Fred S. Goulding

Lawrence Berkeley Laboratory
University of California
Berkeley, California 94720

ABSTRACT

The bimodal particle size distribution in the urban aerosol suggests the use of a dichotomous sampling method with a cut point near two microns. The collection of the two size fractions separately should aid the identification of pollutant sources and the evaluation of fine particle-related health hazards. We have constructed such a sampler in which size segregation is effected by inertial impaction across a virtual surface into a volume of relatively stagnant air. Following a two stage separation, the particle size fractions are deposited on membrane filters. One filter collects 95% of uncontaminated fine particles while the other collects all of the coarse particles along with 5% of the fine fraction.

The sampling scheme is tailored to match the requirements of elemental analysis by X-ray fluorescence and total mass measurements by beta gauging. The design parameters of the virtual impactor have been optimized for minimum loss and sharp cut characteristics. A servo flow controller is utilized to maintain a constant sampling rate of 50 ℓ/min with a particle size cut at 2.4 μm Stokes' diameter. Fully automated units have been developed for a computer controlled monitoring network.

The compatibility of the virtual impactor with other analytical instrument and its adaptibility to automation suggest that it may be suited for wider use.

---

* This work was supported by the Environmental Protection Agency under Interagency Agreement with the U. S. Energy Research and Development Administration.

DICHOTOMOUS VIRTUAL IMPACTORS FOR LARGE SCALE MONITORING OF AIRBORNE PARTICULATE MATTER

Billy W. Loo, Joseph M. Jaklevic, and Fred S. Goulding

Lawrence Berkeley Laboratory
University of California
Berkeley, California 94720

INTRODUCTION

Airborne particulate matter consists primarily of natural aerosols such as soil dust, pollens and sea spray as well as a multitude of man made pollutants in the form of hydrocarbons, sulphates, nitrates and a broad spectrum of trace elements, many of which are considered potentially toxic. Any effective air quality control strategy must be based on detailed knowledge of the generation, transformation, dispersion and depletion of those undesirable substances. Since gas-particle interaction is recognized to play a key role in forming secondary aerosol from primary pollutants, the study of particulate pollutant is an important facet of the total problem.

Unfortunately the problem is made unwieldy by the complex meteorological, geographical conditions and anthropogenic processes. The system under study has no steady state. Any comprehensive air pollution study will require the large scale deployment of instruments to provide both time and position data on the concentrations of the polluting species so that practical models of the systems might be developed.

Energy dispersive X-ray fluorescence analysis has now emerged as a potent and versatile technique for trace element analysis due to its capability for simultaneous rapid multi-element analysis. Quantitative non-destructive analysis on a large and economical scale is possible for most elements of interest[1]. A fully automated analysis system can measure 35 elements ranging from Al to Pb collected on two-hour air filter samples through a sequence of three five-minute runs with a detection limit on the order of 10 ng/m^3 [2]. Such a system can comfortably analyze some 20,000 samples a year.

In understanding the evolution of pollutants and in assessing potential hazards, it is desirable to obtain particle size information in addition to elemental concentrations. It has been observed that urban aerosols tend to have a bimodal size distribution with a minimum at about 2 μm, Whitby, et al[3]. The fine particle fraction peaks at about 0.3 μm and is considered primarily to be the accumulation of combustion products by condensation and coagulation. The coarse particle fraction consists mainly of mechanically produced aerosol with particle size peaking around 10 μm, although this is subject to large fluctuations caused by gravitational settling and impaction losses. There appears to be little mass transfer between the two modes[4]. The occurance of a fairly distinct minimum may correspond to a natural physical effect since the creation of larger surface areas by mechanical means becomes energetically unfavorable at sub-micron sizes. Further interest in separating particles whose sizes lie on either side of the 2 μm point arises because the deposition and retention of aerosols in the human respiratory system is such that particles smaller than 2 or 3 microns are not efficiently removed in the nasal-pharyngeal region and penetrate to the tracheo-bronchial and pulmonary regions[5]. The large surface area (some 60 m^2) in the lungs renders the human body vulnerable to sub-micron pollutants. The coincidence of the size transition at 2 μm in both the particle production and the health effects is a prime motivatoin for developing a dichotomous sampler to collect size-segregated fractions from each size range for subsequent X-ray fluorescence analysis.

OBJECTIVE

As part of the St. Louis Regional Air Pollution Study (RAPS), a network of 25 monitoring stations (RAMS) has been set up to collect meteorological, gaseous and particulate pollutant data. The initial plan called for the installation of automated dichotomous air samplers (ADAS) in ten of these stations to be operated under the control of a central computer. Figure 1 illustrates an integrated program of sampling and analyzing some 20,000 samples per year. To facilitate data handling, each filter carries a computer readable digital label. Total mass loading on filters will be determined by beta-gauge measurements before and after exposure and elemental analysis will be performed by X-ray fluorescence analysis. These results will then be merged with meteorological and other relevent data for inclusion in the main data bank.

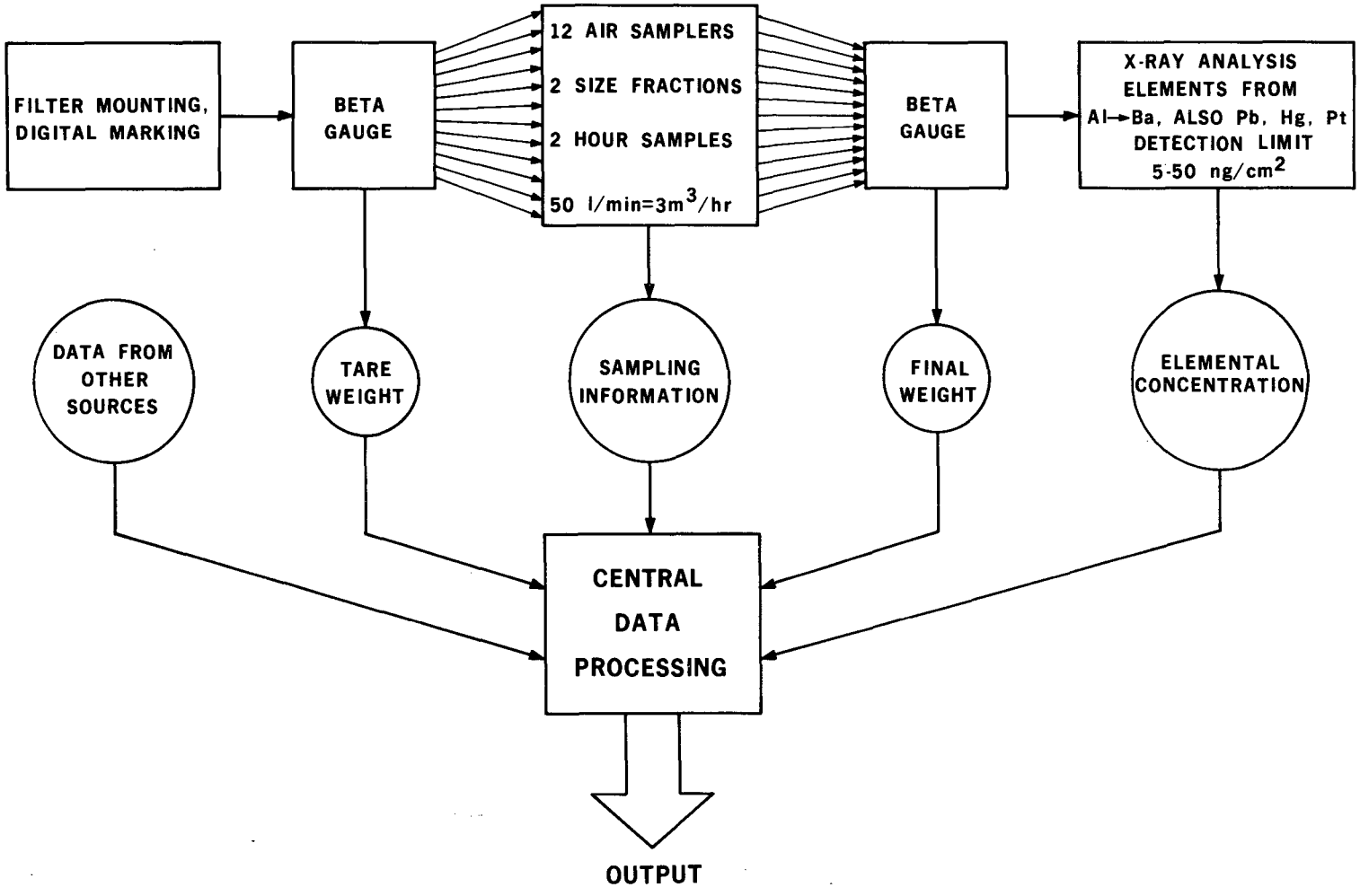

XBL 743-538

Fig. 1 Block diagram of a sampling and analysis system.

Our objective was to develop a dichotomous sampler that matches the requirements of analysis systems. It should collect uniform depositions on a thin substrate of low atomic number and should exhibit a sharp particle size cut with very small or zero particle losses in the apparatus. It should provide a high sampling rate to permit adequate sample collection in a reasonably short time. Ease of sample handling and reliable operation are also very important considerations for large scale monitoring. The desired sampling rate and particle size cut point have been chosen to be 50 ℓ/min and 2 μm respectively.

APPROACH

One of the prime considerations in particle sizing is the selection of a physical mechanism by which size separation can be accomplished. Since the shape, density and dielectric properties of the atmospheric aerosols cannot be predicted, the interpretation of the term "particle size" depends largely on the method of measurement. Since effects of particulates depend on their transport processes in the atmosphere and on their uptake and retention through respiration, inertial methods of separation should provide more relevant data than electrical, thermal or optical methods. We shall therefore regard the size of a particle as being the diameter of an aerodynamically equivalent unit density sphere (i.e., the Stokes' diameter).

Conventional methods of inertial separation in the 2 μm range often uses an impactor which is an air jet impinging on a collection plate as shown in Fig. 2. The jet size, velocity and geometry are controlled so that the inertia of particles above a certain size causes them to overcome the drag force as they leave their deflected stream lines and to impact onto the plate. A useful concept in impactor studies is the Stokes' number Stk defined as

$$\mathrm{Stk} = \frac{\rho_p C V_o D_p^2}{9 \mu D_1} \qquad (1)$$

where ρ_p = particle density

C = Cunningham slip correction for the discontinuous nature of fluid interaction when the pressure is low or when the particle size is small compared with the molecular mean free path in air

V_o = mean fluid velocity of the jet

D_p = particle diameter

μ = viscosity of air

D_1 = a characteristic size usually taken as the jet diameter.

At low Reynolds' numbers, the drag force on a particle is $3 \pi \mu V D_p$ as given by the Stokes' law, where V is the relative velocity between the fluid and the particle. The Stokes' number is a measure of the ratio of inertial force (in this case centrifugal force) to the drag force. It is also equal to the stopping distance of a particle in stagnant air divided by the jet diameter. Under a given set of flow conditions, particles with a Stokes' number higher than a critical value are impacted onto the collection plate. It can therefore be regarded as useful for scaling purposes.

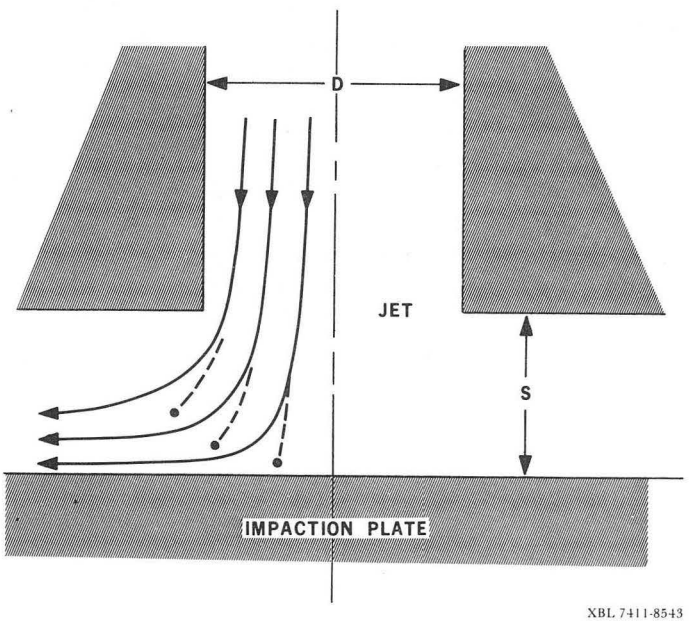

Fig. 2 Schematic of a conventional impactor

Impactors with one or more size cuts have been widely used for collecting size-segregated particulate samples. However, the inherent difficulties with particle bounce, reentrainment, non-uniform deposition and cumbersome sample handling have limited their potential for large scale applications. A virtual impactor uses the principle of inertial separation, but the impaction plate is replaced by a region of relatively stagnant air (receiving tube in Fig. 3 and 4). The virtual surface formed by the deflected streamlines realizes similar boundary conditions to those in real impactors. Large particles will pass into the forward low-flow region while small particles will remain mostly in the high-flow air stream deflected radially around the receiving tube. Both size fractions can subsequently be deposited onto separate filters.

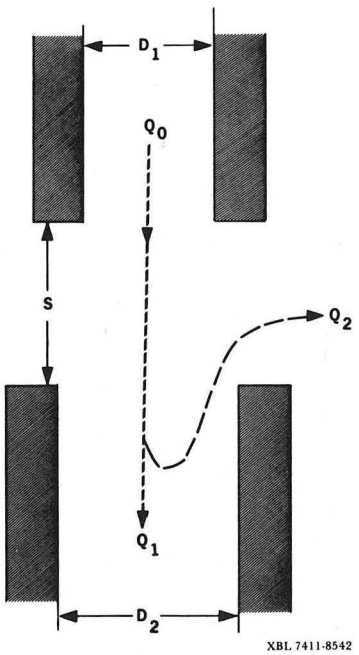

Fig. 3 Critical parameters of a virtual impactor

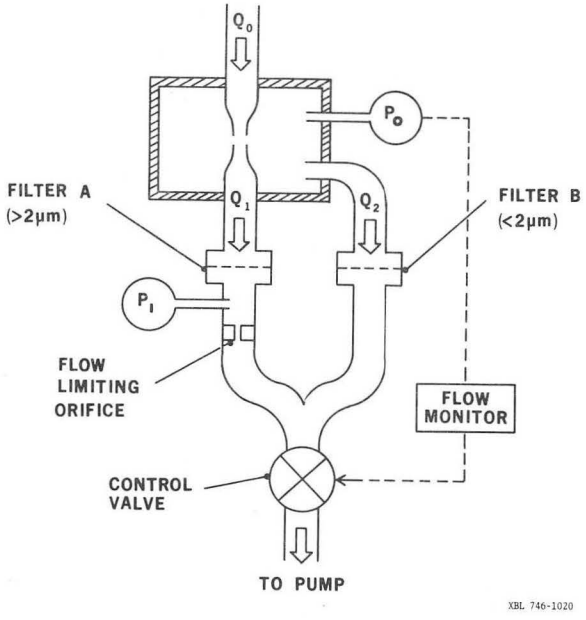

Fig. 4 Schematic of a single-stage dichotomous virtual impactor

A virtual impactor possesses several distinct advantages:

1) Particle depositions on the filters can be made quite uniform, which is ideal for photon excited X-ray fluorescence analysis and total mass measurement using a beta gauge.

2) The size and pattern of deposition can be controlled to match the optimum requirement of the analysis system.

3) Since the object is to avoid collection within the apparatus, particle bounce is a favorable phenomenon. In fact it is desirable to shape streamlines as nearly tangential to the surfaces as possible to encourage bounce and thereby reducing losses.

4) Reentrainment of particles in the air stream is a second order effect since only particles lost in the apparatus are subject to blow off.

5) Collecting samples external to the apparatus not only facilitates automatic sample handling but also permits the design of the impaction geometry to concentrate on maintaining precise and consistant separation characteristics.

6) The virtual impactor can serve as an input stage for any downstream instrument.

VIRTUAL IMPACTOR DESIGN CONSIDERATIONS

An early study of a virtual impactor was done by William Conner[6], who utilized ideas from the cascade centripeter[7]. Although the measurements and analysis were inaccurate, it did demonstrate the size separating power of the virtual impaction principle. A more sophiscated version using two cascade separation stages was developed by Carl Peterson of the Environmental Research Corporation. We have made a detailed evaluation on the ERC unit to assess the feasibility of the virtual impaction scheme for large scale sampling[8]. Emphasis in our work has been placed on improving the sharpness of the particle size cut characteristics and reducing losses. The result of this and other related studies revealed the importance of several factors which govern the performance:

1) Jet Reynolds' number - The Reynolds' number is defined as $\rho VD/\mu$, where ρ and μ are the density and viscosity of air and V is the mean air velocity and D is the diameter of the jet. Excessive turbulence which tends to occur at high Reynolds' numbers sets an upper limit to the maximum flow in a jet for a given size cut.

2) Flow symmetry and alignment - The sharpness of the cut characteristic is degraded by the azimuthal flow asymmetry about the axis of each jet. In our design this effect is minimized. It is clear that rectangular jets have inferior performance in this regard and stable symmetrical flow configurations are difficult to maintain. The coaxial alignment of jet and receiving tube is obviously essential.

3) Flow control - A feedback system is needed to maintain a constant operating point independent of variations in the filter impedance (including changes due to particle loading).

4) Particle bounce - Taking advantage of the non-sticking probability of solid particles, streamlines are designed to be as nearly tangential to the physical surfaces of the impactor as

is possible. Contours of parts are shaped to reduce impaction losses.

5) Critical parameters - Referring to the notations in Fig. 3 on the relevant parameters of a simple jet and impaction tube, it is necessary to determine an optimum set of parameters Q_0, D_1, Q_1/Q_0, D_2/D_1 and S/D_1 for minimum loss at a given size cut. A fundamental study of conventional impactors has been done by Marple[9]. However, the theoretical analysis is not readily applicable to the case of the virtual impactor due to the much more complex boundary conditions. We have adopted an empirical approach, first measuring the range and sensitivity of each parameter then converging onto a region where the cut point is relatively definitive and stable and where remaining parameters are optimized.

METHODS OF MEASUREMENT

Due to the close approximation of their geometric diameters to unit density Stokes' diameters, dioctyl phthalate (DOP) droplets are well suited as test particles. Particles between 1 to 10 μm in size can very readily be produced in a Berglund-Liu monodisperse aerosol generator with uranine (fluorescein sodium) used as a tracer for quantitative measurements. The generator utilizes the uniform breakup of a liquid jet into droplets as it passes through a vibrating orifice. The final size of a liquid or solid particle is calculated from the initial solvent concentration, jet flow rate and vibration frequency. The monodisperse aerosol output is then used to test a particular impactor configuration. Particle depositions can be dissolved in water and the uranine content of the solution determined by UV fluorescence techniques. Such procedures to determine deposits on parts have been described in detail in an earlier report[8].

The Stokes' diameters of solid particles are less well defined because of uncertainties in the final density of the particles. Figure 5 is a picture of an "8.8" μm NaCl particle as viewed by a scanning electron microscope at 7000 magnification. The void fraction after the solvent is evaporated is estimated at 50%. The sizes of solid particles (uranine) used in our final evaluation were assigned using the size cut characteristics of the virtual impactor as measured with liquid DOP particles in order to compensate for such uncertainties.

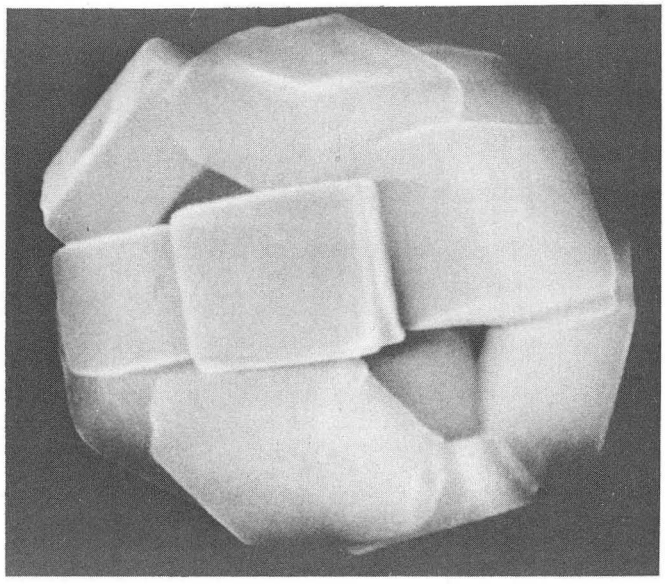

Fig. 5 A "8.8" μm NaCl particle as viewed by a scanning electron microscope.

Flow measurements were made with pressure-corrected rotameters and cross checked with a temperature-compensated integrating flow meter. All calibrations were performed at 20°C and 735 mm Hg pressure.

We shall now digress to a problem of special interest which is the measurement of the flow division within a two-stage virtual impactor where the internal flows are not directly assessable. Referring to the schematics of a two-stage virtual impactor (Fig. 15), the flow conditions may be closely approximated by the equivalent circuit shown in Fig. 6. R_0, R_1 and R_2 represent the non-linear flow impedances associated with the inlet orifice, and the orifices in the coarse and fine particle streams respectively. The flow division Q_1/Q_0 may be derived from the measurement of the total external flow as a function of a single static differential pressure P_0 between the inlet and the second stage of the impactor as shown in Fig. 7. Curve A is the characteristic when R_1 and R_2 are made zero by removing the inner section of the virtual impactor. Curve B is the characteristic with all the parts in place and Curve C is similar to B except that R_1 is made infinite by temporarily sealing the orifice such that R_0 and R_2 are in

series. Under normal operation, the total flow is Q_0 and XY is the pressure differential across R_2. Hence, Q_2 is determined graphically by locating UV = XY. In this case Q_1/Q_0 is measured to be 24.9%.

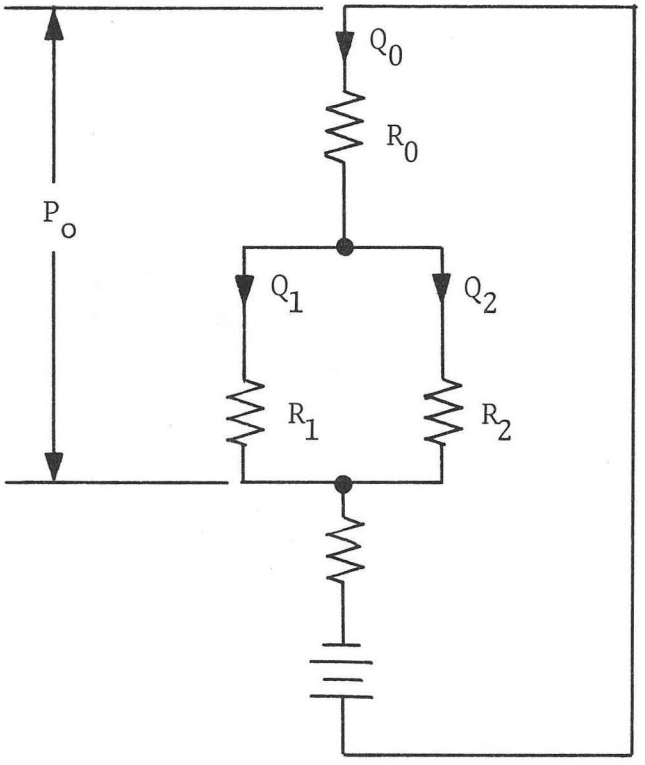

Fig. 6 An equivalent circuit of fluid flow in a virtual impactor.

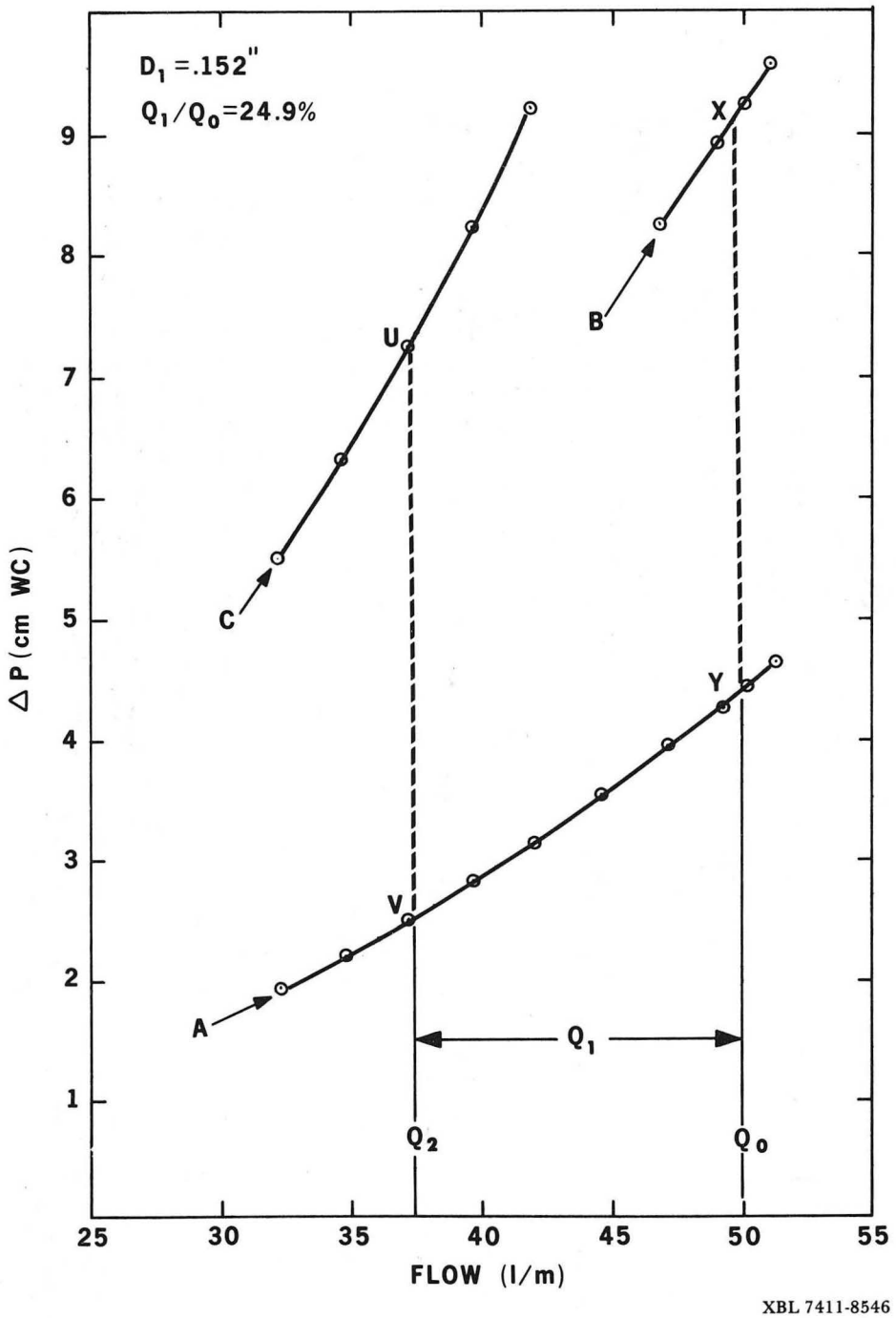

Fig. 7 A graphical solution to the internal flow distribution problem in a two-stage virtual impactor.

RESULTS AND DISCUSSION ON DESIGN STUDIES

A series of measurements have been made to probe the behavior of a single-jet virtual impactor. The coarse and fine particles were collected on filters A and B corresponding to greater and less than 2 μm respectively. For each set of measurement, the collection efficiency, defined as E = A/(A+B), and/or particle losses were observed as a function of the parameter being varied. Starting with a set of parameters near the 2 μm cut point, the objective was to develop an optimum set of parameters with a minimum number of excursions in the multiparameter space. The selection of 2 and 10 μm test particles were used as fiducial sizes in this regard.

The results of such measurements are shown in Figs. 8 through 14. Table 1 is a summary of the conditions under which each profile is observed, using the symbols of Fig. 3.

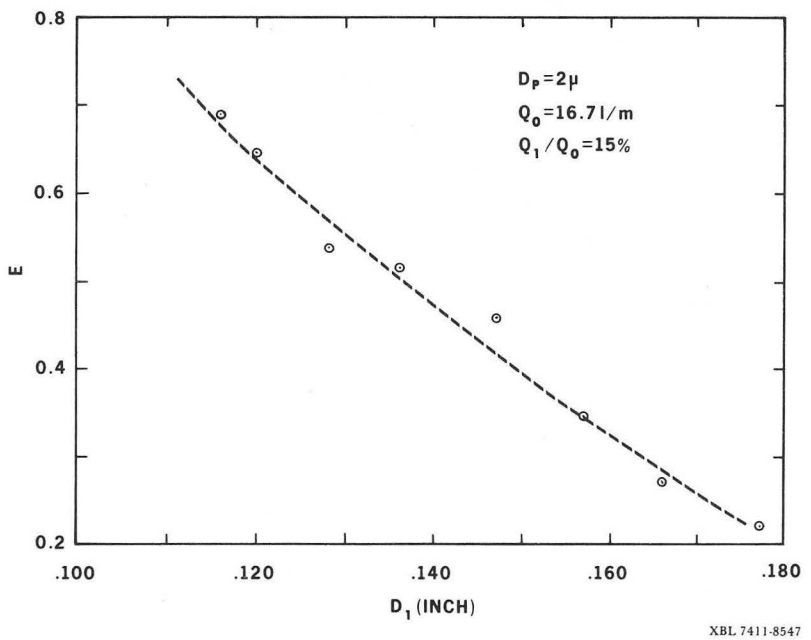

Fig. 8 Behavior of E vs. D_1

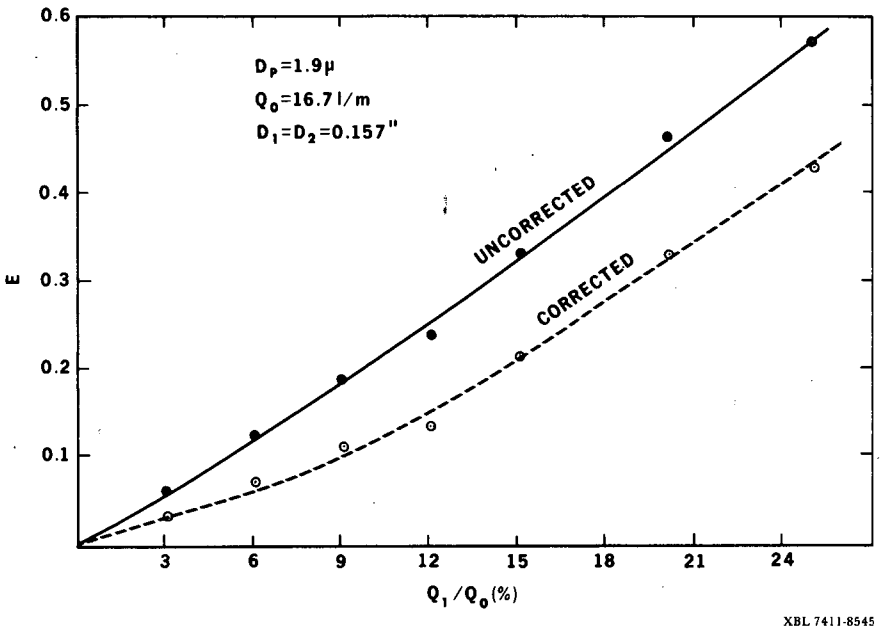

Fig. 9 Behavior of E vs. Q_1/Q_0

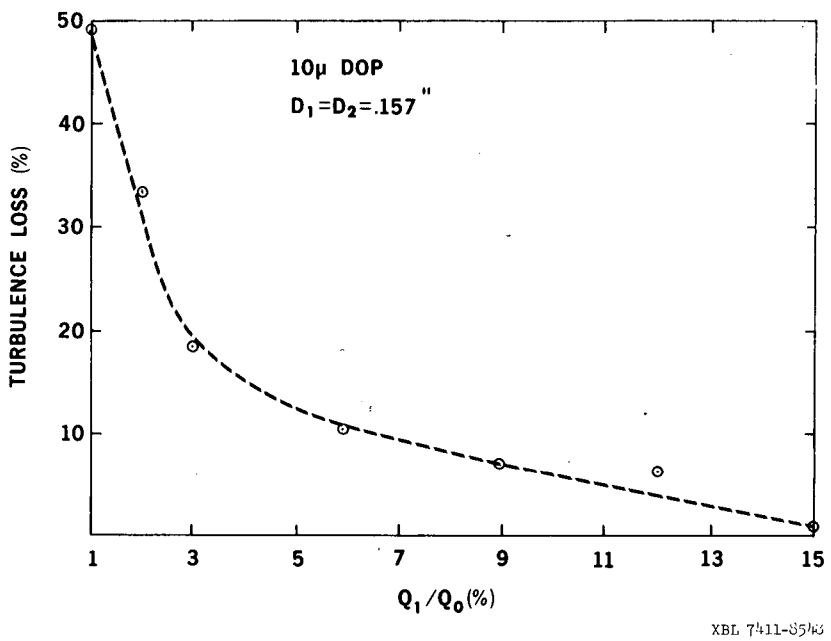

Fig. 10 Turbulent mixing as a function of Q_1/Q_0

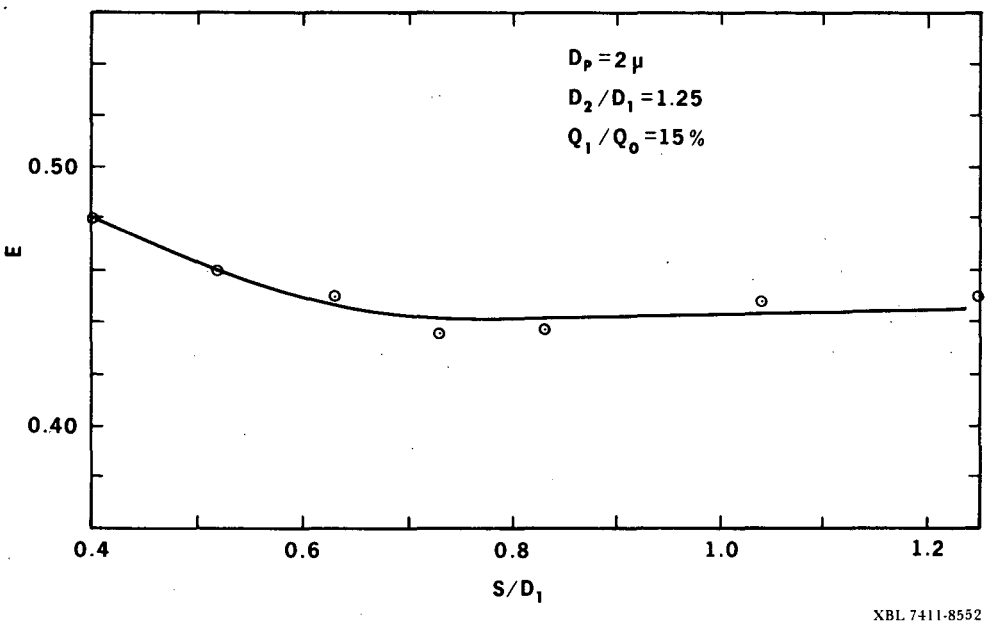

Fig. 11 Behavior of E vs. S/D_1

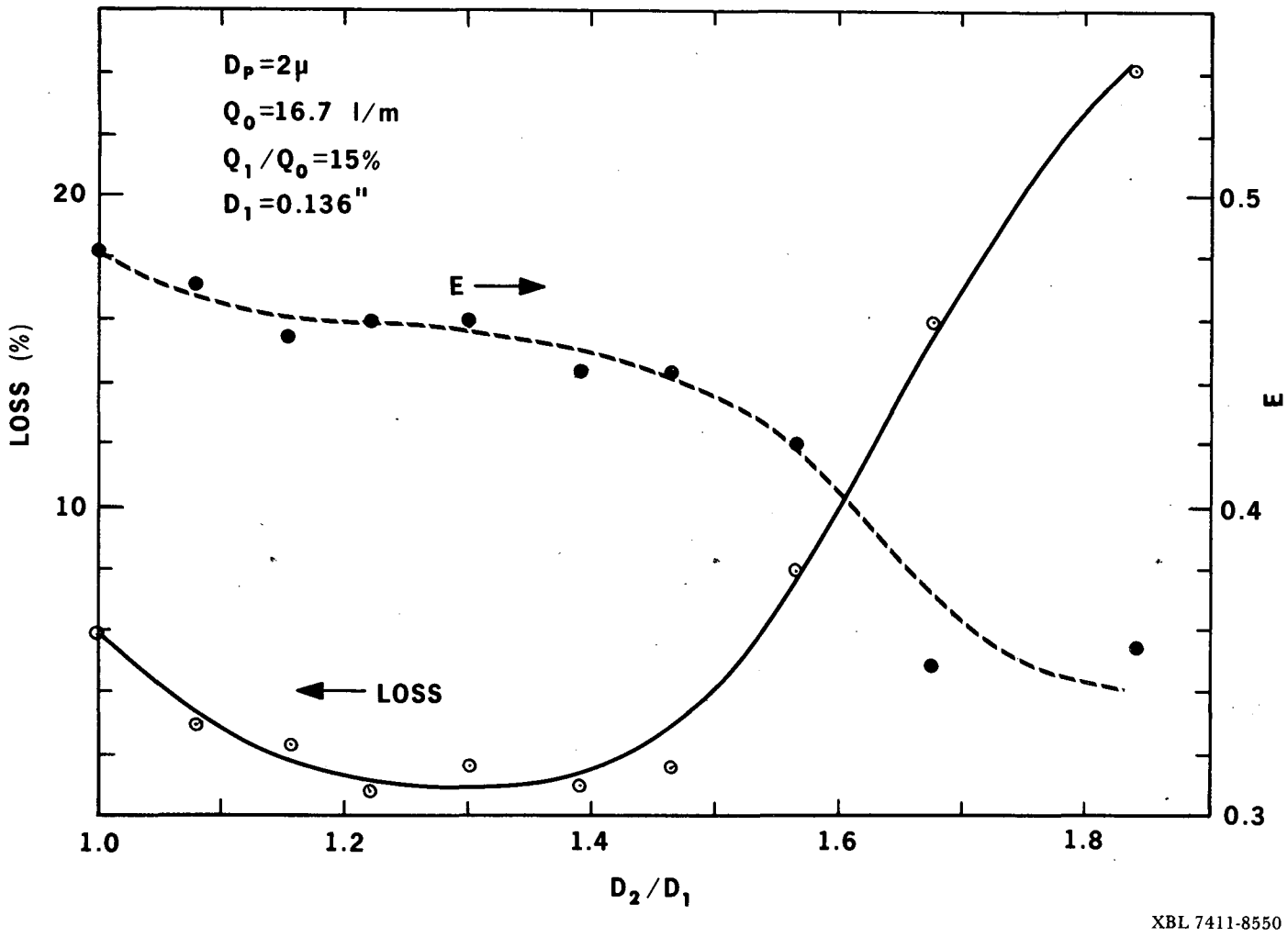

Fig. 12 Behavior of E and losses vs. D_2/D_1

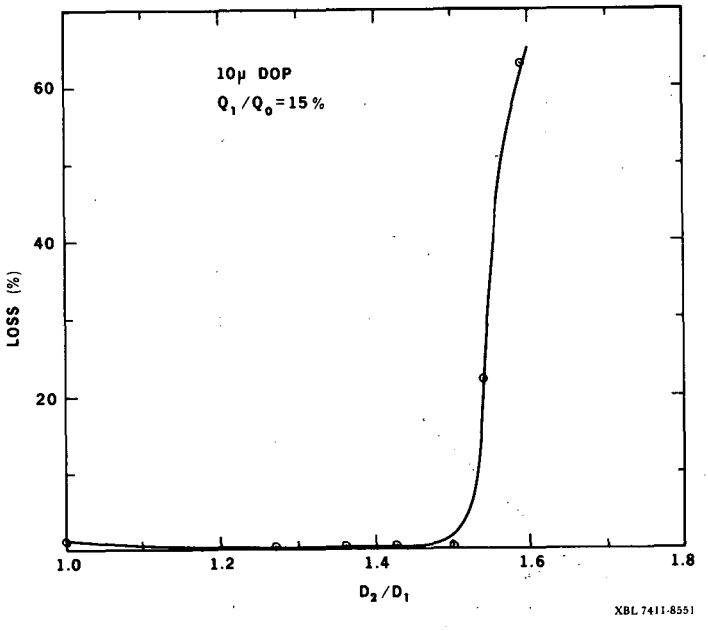

Fig. 13 Losses of 10 μm DOP particles as a function of D_2/D_1

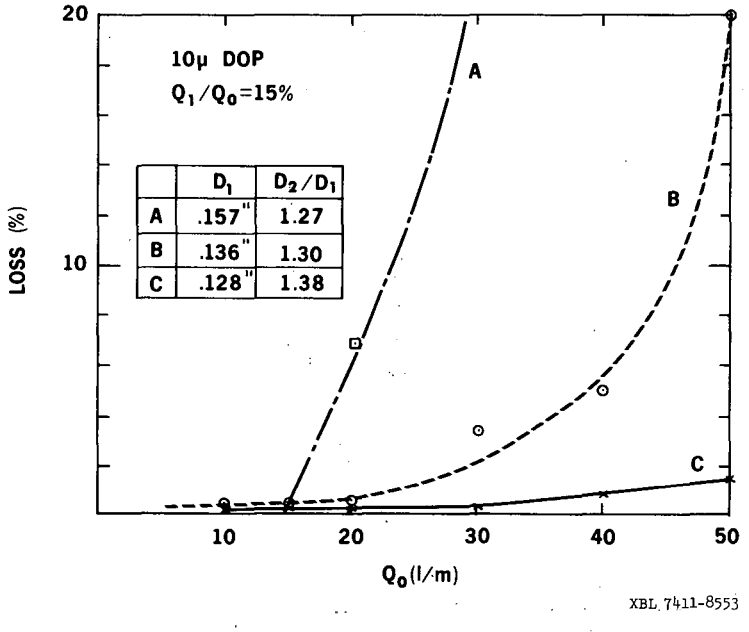

	D_1	D_2/D_1
A	.157"	1.27
B	.136"	1.30
C	.128"	1.38

Fig. 14 Losses of 10 μm DOP particles as a function of Q_0

FIGURE NO.	DEPENDENT VARIABLE	Q_0 (ℓ/m)	Q_1/Q_0 (%)	D_1 (mm)	D_2/D_1	S (mm)	D_p (μm)	PARTICLE
8	E	16.7	15	VARIABLE	1.0	3.2	2	URANINE
9	E	16.7	VARIABLE	4.0	1.0	4.0	2	URANINE
10	LOSS	16.7	VARIABLE	4.0	1.2	3.5	10	DOP
11	E	16.7	15	4.0	1.0	VARIABLE	2	URANINE
12	E	16.7	15	3.5	VARIABLE	3.2	2	URANINE
12	LOSS	16.7	15	3.5	VARIABLE	3.2	2	URANINE
13	LOSS	16.7	15	4.0	VARIABLE	3.2	10	DOP
14	LOSS	VARIABLE	15	4.0 3.5 3.3	1.27 1.30 1.38	3.2	10	DOP

TABLE 1 Summary of conditions underwhich initial virtual impactor testings were conducted

Figure 8 shows the variation of E with D_1. This strong dependence on jet velocity is expected to be the dominant factor governing the cut point. Figure 9 shows the variation of E with the flow division Q_1/Q_0. The corrected values of E, after contamination of fine particles in the coarse particle stream has been subtracted, indicate the need for a significant amount of flow in the forward direction, particularly for the particles near the cut point. At a given Q_1/Q_0 there will always be the same fractional contamination of fine particles in the large particle stream but more than one stage of separation can be used to reduce this below the amount desired. The results in Fig. 10 were taken with a single-stage virtual impactor with three jets in parallel. The cross-contamination of 10 μm particles in the fine particle stream is taken as a measure of turbulent mixing. It is obviously desirable to use a value of Q_1/Q_2 greater than 15% for each stage of separation.

The dependence of E on the spacing S between the inlet jet and the receiving tube is shown in Fig. 11. It is seen that E is about constant for S/D_1 greater than 0.5.

Figure 12 shows both E and the losses as a function of D_2/D_1. Note that E has a flat region for $1.1 < (D_2/D_1) < 1.5$ and the impaction loss on the lip of the receiving tube has a pronounced minimum at $D_2/D_1 = 1.3$ and increased rapidly beyond 1.5. The same sharp increase in losses at $D_2/D_1 \simeq 1.5$ is also observed (Fig. 13) for 10 μm particles, suggesting that this extreme sensitivity is related to flow geometry rather than to particle size. This may explain the poor performance of virtual impactors with a rectangular slit geometry.

All these measurements were taken with the assumption that a total flow rate of 50 ℓ/min will be drawn through three inlet jets in parallel to achieve a cut point at 2 μm and the jet Reynolds' number will typically be in excess of 5000. For best performance Marple has shown that the optimum jet Reynolds' number is about 3000 for a conventional impactor. Figure 14 illustrates the effect of particle losses as Q_0 is increased. It appears that the wall losses are the result of the increase in stopping distance of the very large particles as they leave the diverging streamlines at the region of separation, although a small component due to turbulence losses has not been ruled out. It might be possible to overcome this impaction loss by using a more complex design of the receiving tube.

The considerations of jet Reynolds' number, flow symmetries, turbulent mixing, stability of the cut characteristic and flow geometry for minimum loss have led to the conclusion that sampling 50 ℓ/min with a 2 μm cut point with a tolerable fine particle contamination in the coarse particle stream requires two series stages of separation with

three parallel jets for the inlet stage and a single jet for the second stage. The appropriate parameters will be $Q_1/Q_0 \geq 15\%$, $D_2/D_1 = 1.3$ and $S \approx 1$.

DESCRIPTION OF VIRTUAL IMPACTOR

The schematic of the complete virtual impactor design is shown in Fig. 15. It consists of the following main components:

PARTICLE SIZE FRACTIONATOR

Details of this component are illustrated in Fig. 16 with the key parts numbered. Air is drawn through three inlet jets (part 1) in parallel. Their protrusion into the first stage cavity is necessary to eliminate the "backwall" losses on part 2 due to the spatial oscillation of streamlines as found in the ERC design, as well as in some conventional impactors. Part 3 forms the first stage cavity. The three small holes in this part are symmetrically located about the central axis but are offset 60° azimuthally with respect to the coarse particle receiving tubes (parts 4) to minimize flow interference. These holes, in combination to the one in part 7, also govern the internal flow distribution. The Q_1/Q_0 for the first stage was adjusted to be 25% to minimize wall losses in the cavity. The tapered lips on the tubes have no significant effect on the cut point although they do tend to defocus the streamlines and reduce cavity losses.

The three coarse particle jets are then converged by a 15° cone (part 6) onto the second stage of separation after passing through the drift tube (part 5). Parts 8 are three positioning rods which forms an open cavity for the second stage jets. The ratio Q_1/Q_0 here is chosen to be 20%. Thus 2.5 ℓ/min of air will pass through filter A carrying all the coarse particles along with 5% of the fine particles. The fine particle stream of the second stage will merge with that from the first stage and be deposited on filter B. In analysis, a correction for the 5% contamination on filter A can be made based on the amount of the uncontaminated 95% of the fine particles on filter B. Table 2 summarizes the actual parameters used.

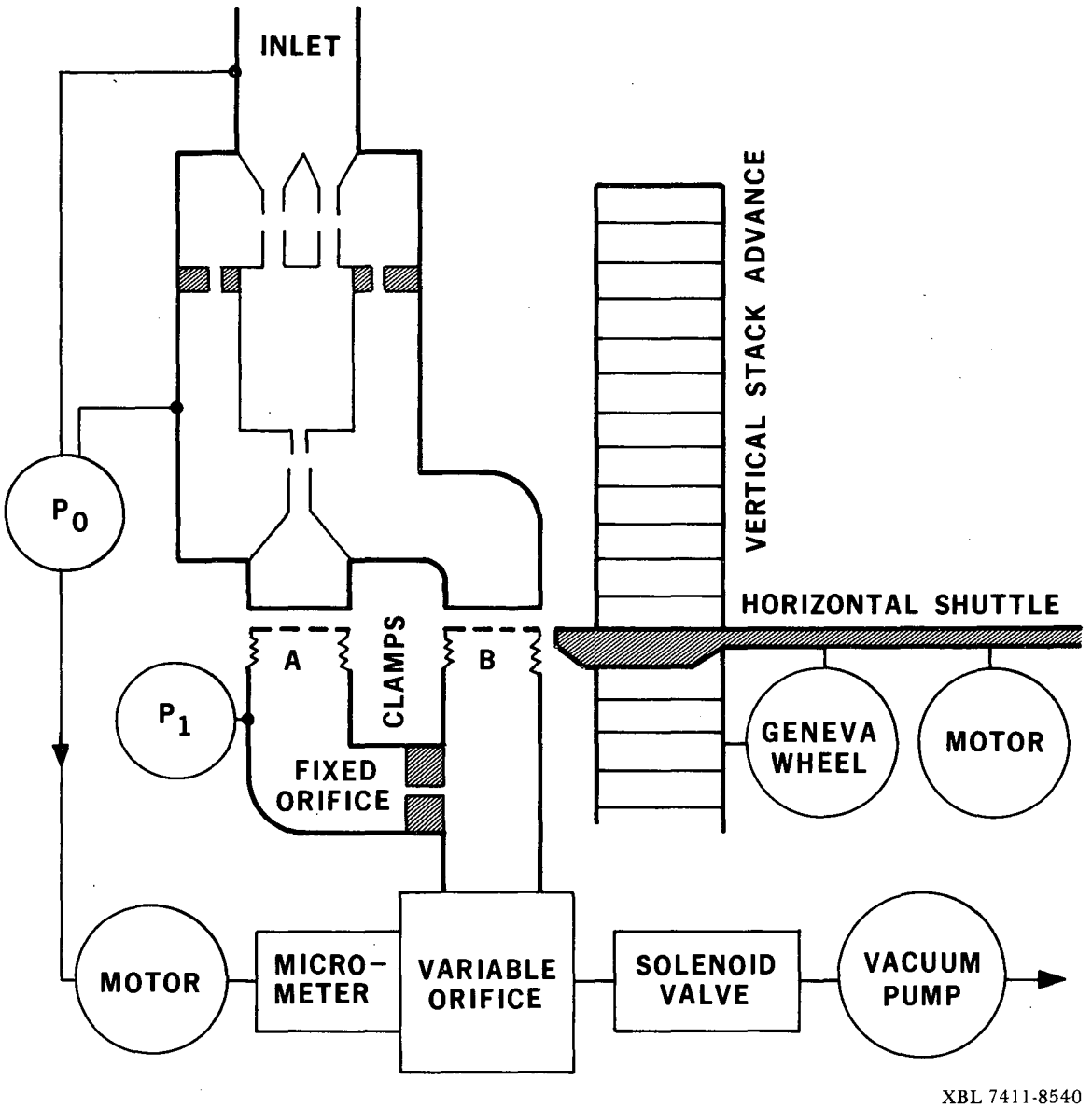

Fig. 15 Schematic of the automated dichotomous air sampler.

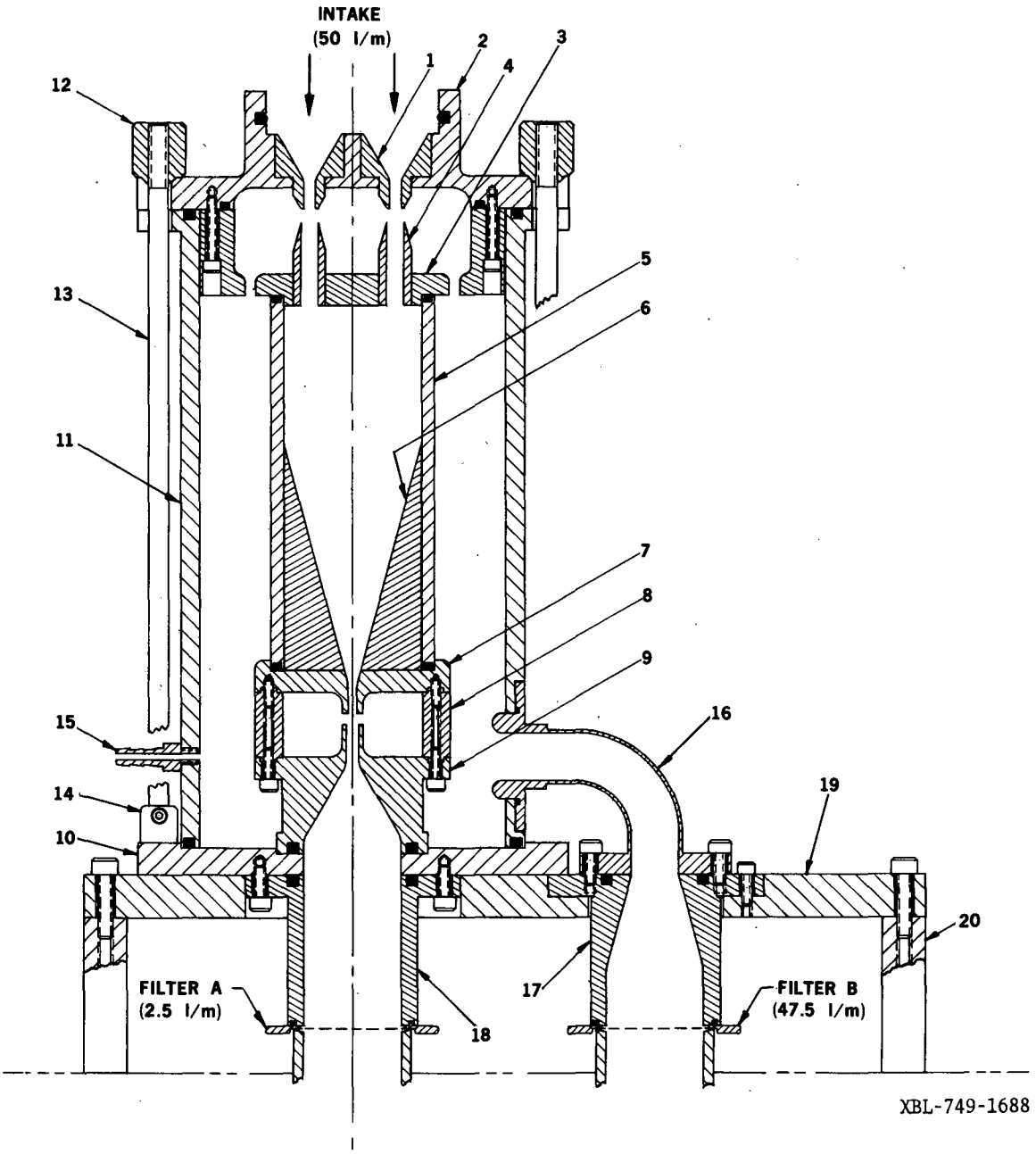

Fig. 16 Details of the virtual impactor.

PARAMETERS	Q_0 (ℓ/min)	Q_1/Q_0 (%)	D_1 (mm)	D_2 (mm)	S (mm)
First Stage Each of 3 Jets	16.7	25	3.86	5.05	3.81
Second Stage Single Jet	12.5	20	2.87	3.86	3.18

Table 2 Final choice of virtual impactor parameters

The overall construction utilizes all stainless steel parts (excepting part 6) for mechanical integrity and corrosion resistance, compression O-ring seals and tie rods (parts 13) with thumb nuts (part 12) for easy disassembly. Strategic corners are shaped to minimize losses. Figure 17 shows the actual components of a virtual impactor.

FLOW CONTROLLER

Flow regulation is essential for precise measurement of the air volume sampled and the maintenance of a fixed particle-size cut point. This is accomplished as shown in Fig. 15 by sensing (through part 15) the pressure differential P_o between the inlet and the second stage of the impactor with a diaphram operated null switch (Dwyer Model 1640-5) which, in turn, causes the opening in a motor driven valve to be increased or decreased to maintain the preset null condition. The valve is simply a 5.1 mm diameter orifice pierced by a travelling micrometer shaft with a 2° taper. A fixed orifice limits the flow through filter A to 2.5 ℓ/min. The variable orifice and the null switch thus form a feedback loop to compensate any impedance change in filter B. The carbon-vane vacuum pump used (Gast Model 0522-103-G18D) has adequate pumping power to overcome an increase of about 70% in impedance from a typical initial value of 26.2 torr-cm^2/ℓ/min (1.2 μm cellulose membrane filter manufactured by Nuclepore Corporation).

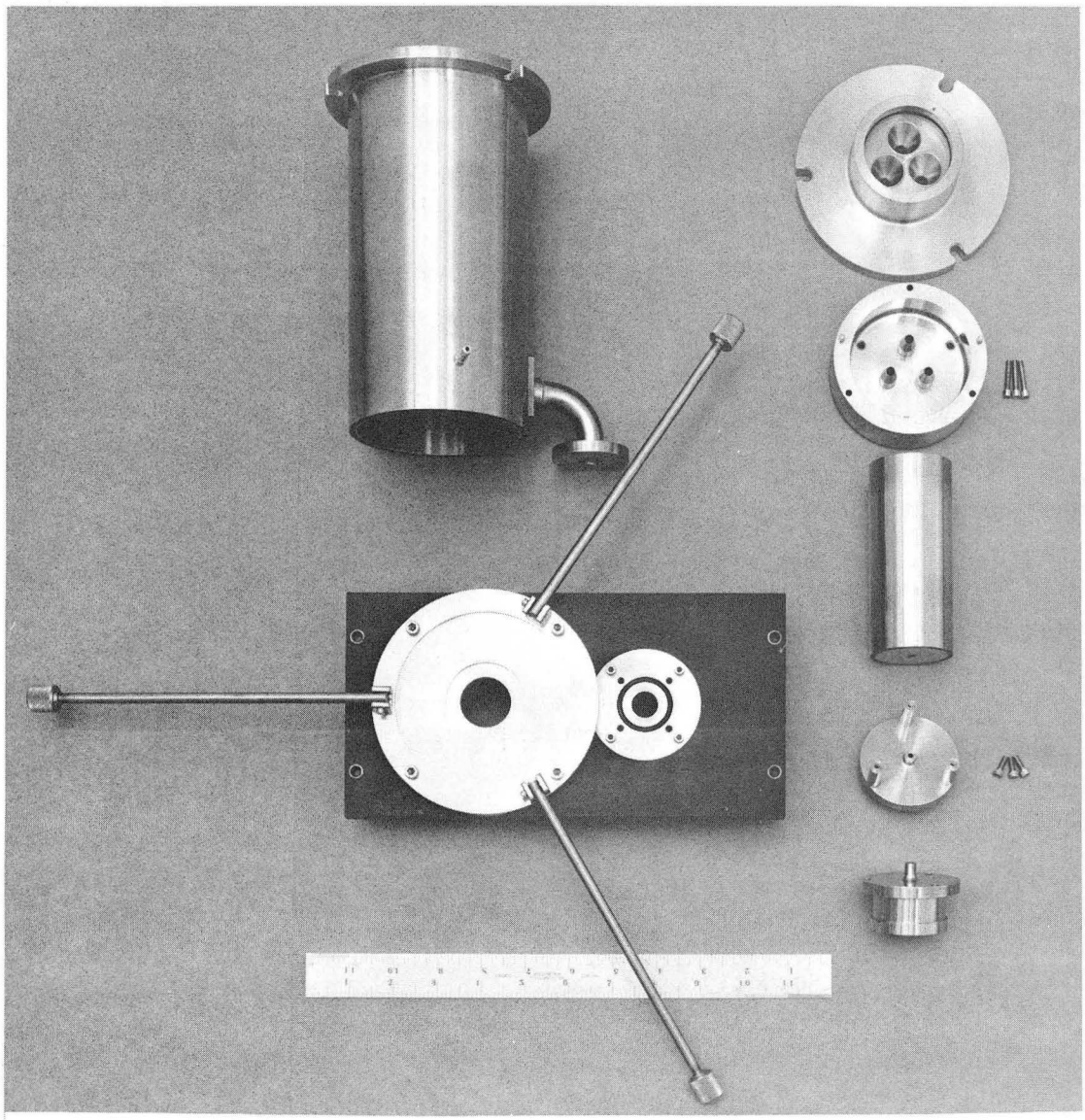

Fig. 17 Disassembled components of the cirtual impactor.

AUTOMATED SAMPLING SYSTEM

Our objective has been to develop a fully automated sampling system for extended continuous operation. It is designed to cycle samples with the minimum amount of handling and preparation. A network of such samplers is to be controlled by a remote computer which also monitors the system status and possible failure modes. Key components include:

FILTERS

The filters used are 37 mm discs of cellulose membrane filters supplied and mounted in 5.1 cm x 5.1 cm plastic frames by the Nuclepore Corporation. Up to 36 of these slides are carried in a linear array in standard 35 mm projector cartridges (Argus Camera). Figure 18 shows such a pair of cartridges containing the digitally labeled filter holders.

SAMPLE CHANGER

The function of the slide changer is to extract a matched pair of filters from side by side slide trays corresponding to the A and B filter stacks, (only one stack is illustrated in Fig. 15). A horizontal shuttle manipulates the slides into their sampling positions where they are clamped in the output tubes of the virtual impactor. Upon the completion of the sampling interval, they are unclamped and withdrawn back into the slide trays. The over-travel of the shuttle actuates a "Geneva wheel" which advances the stack by one vertical increment to be ready for the next insertion. A single motor drives the shuttle which performs the function of transporting, clamping and unclamping slides together with advancing the trays with a single forward and return stroke.

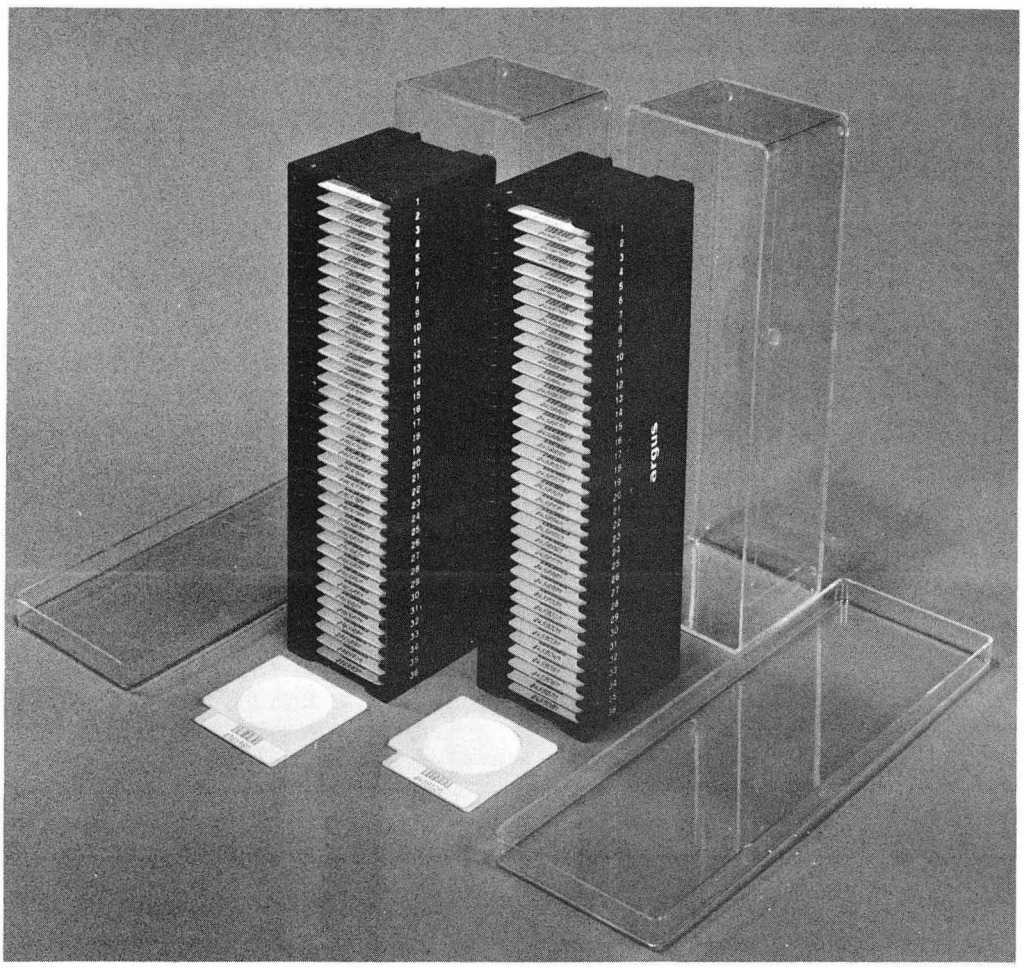

Fig. 18 Typical slides and slide trays used in automated samplers.

FLOW MONITOR

Several types of out-of-range conditions in the flow circuit are detected and indicated by the system. Excessive travel of the micrometer valve due to the presence of leaks or broken filters causes out-of-range switches to be activated. An auxiliary pressure sensing snap switch P_1 (Fig. 15) is used to detect improper clamping or a broken filter. Since the vacuum needed for the fixed limiting orifice results from the proper flow condition in the fine particle stream, P_1 actually monitors the conditions at filter B even before the micrometer valve reaches its limits.

ELECTRONIC CONTROLLER

The selection of sampling intervals, execution of the sequential steps, regulation of flow, detection of errors, monitoring and display of the system status and communication to an optional remote computer are performed via the control module shown in Fig. 19.

In order to maintain the synchronism of the samplers with the clock, ten seconds are allowed for a sample insertion or withdrawal cycle, which normally requires about seven seconds, to complete. Figure 20 illustrates the time sequence of a typical sampling period. While the vacuum pump is turned on continuously, actual sampling starts at the twenty second mark when a solenoid valve is opened. Another ten seconds are allowed for steady flow conditions to be established before the flow controller is enabled. The right hand column of the figure indicates the sequence in which error conditions are checked. The maximum times allowed to complete a sample transport and flow adjustment are 10 seconds and 12 minutes respectively.

To ensure synchronization in the event of short ac power failures (< 10 min) the elapsed time clock and logic control circuits are automatically switched to a rechargeable battery.

Figure 21 shows a complete sampler. It is contained in a portable soundproofed electronic rack with a plastic dust cover and a special inlet pipe designed to draw an isokinetic sample from a larger rooftop sampling port. Figure 22 is a closer view of a sampler with the dust cover removed. It shows the final modification of adding a 7.6 cm section to the height of the virtual impactor to reduce losses in the drift tube.

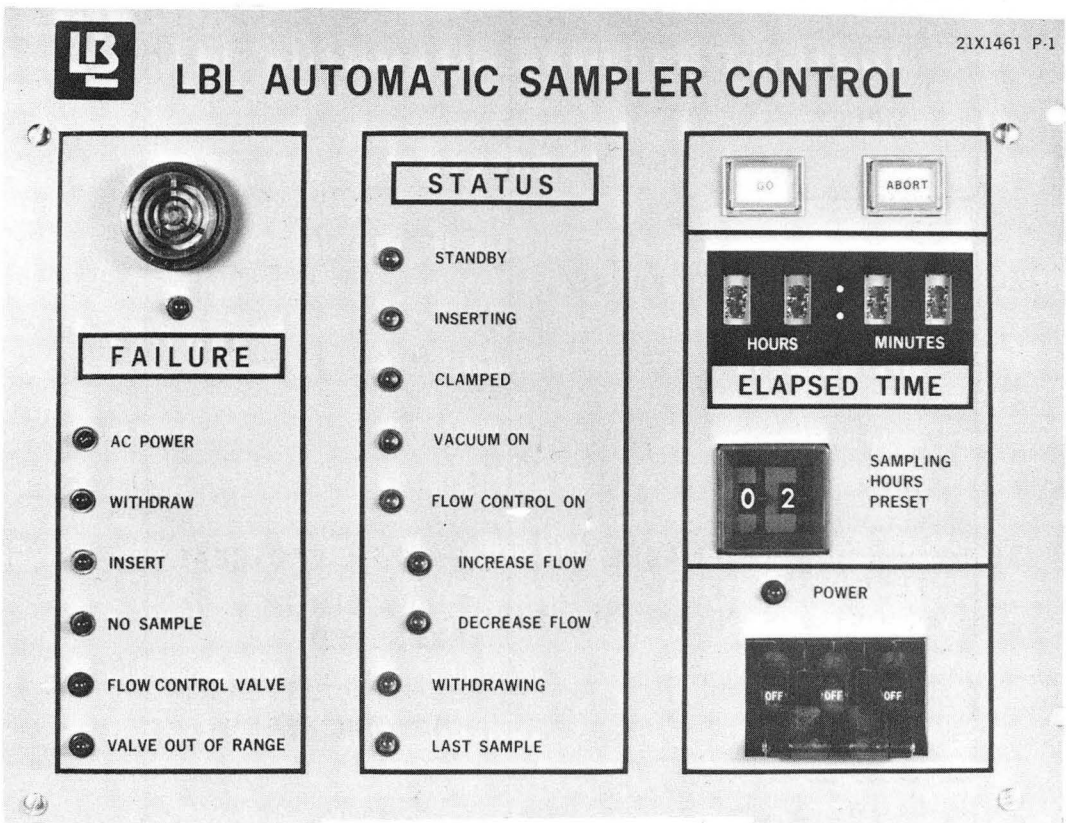

Fig. 19 Front panel of the electronic controller.

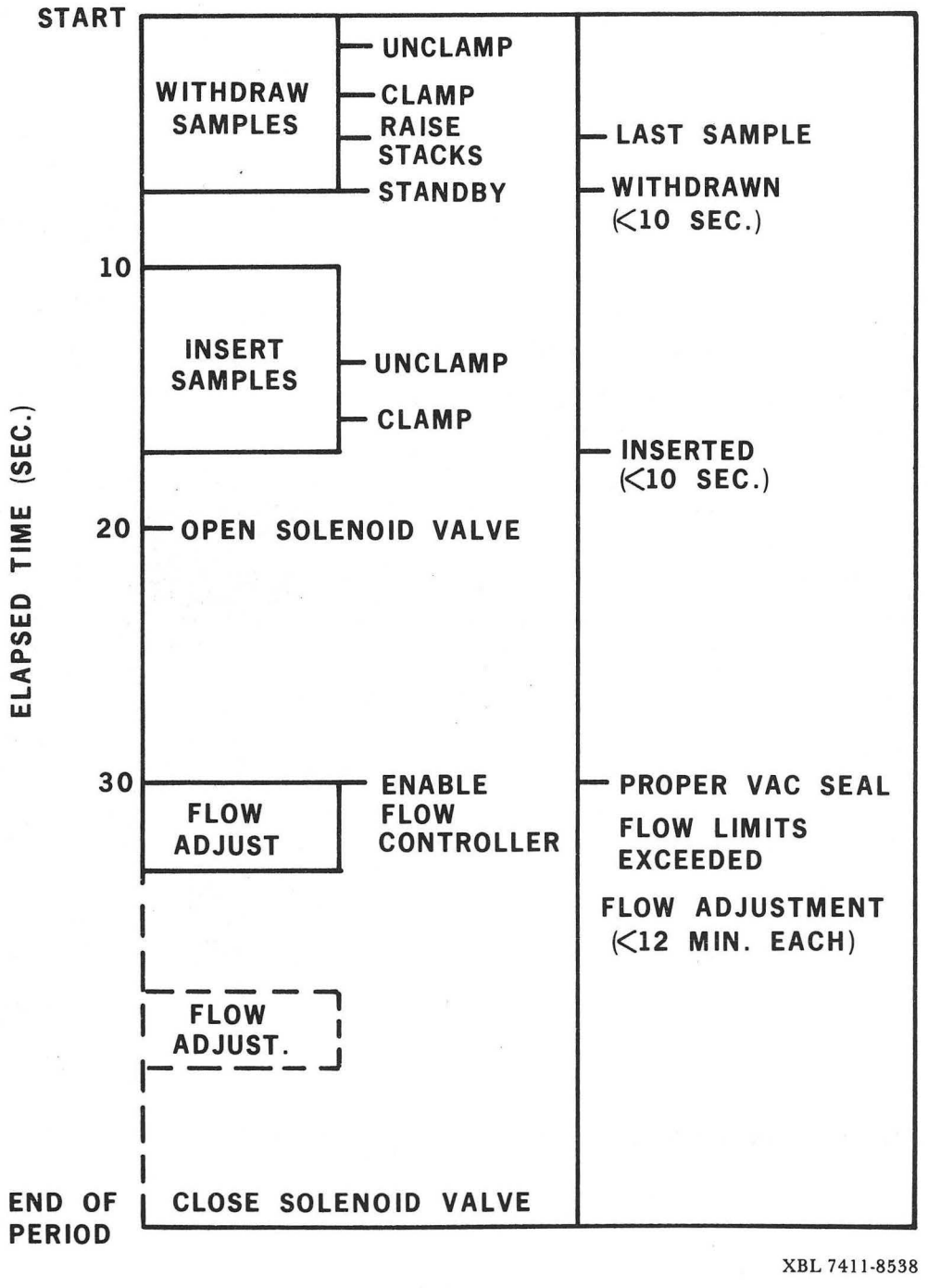

Fig. 20 The functional time sequence of a sampling period.

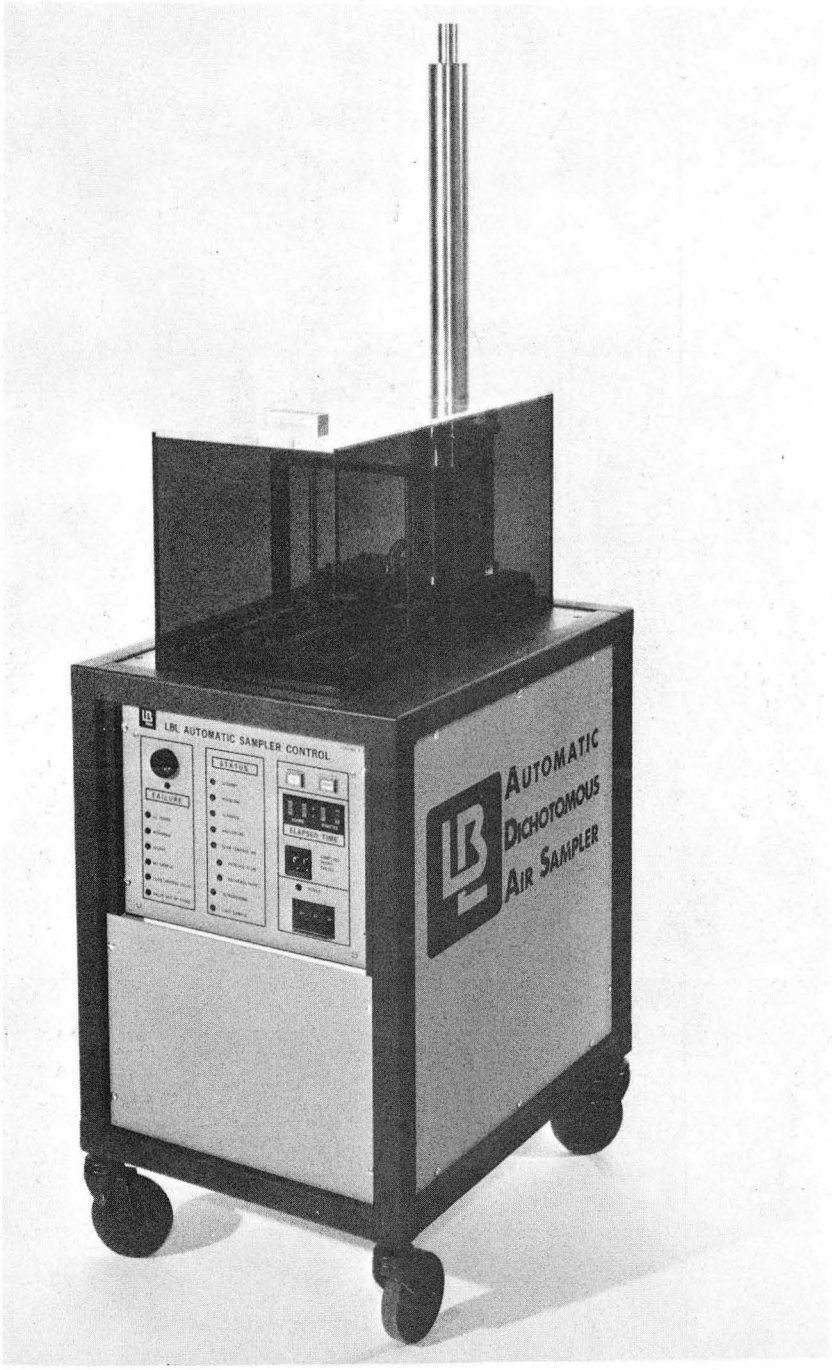

Fig. 21 Oblique view of a completed ADAS.

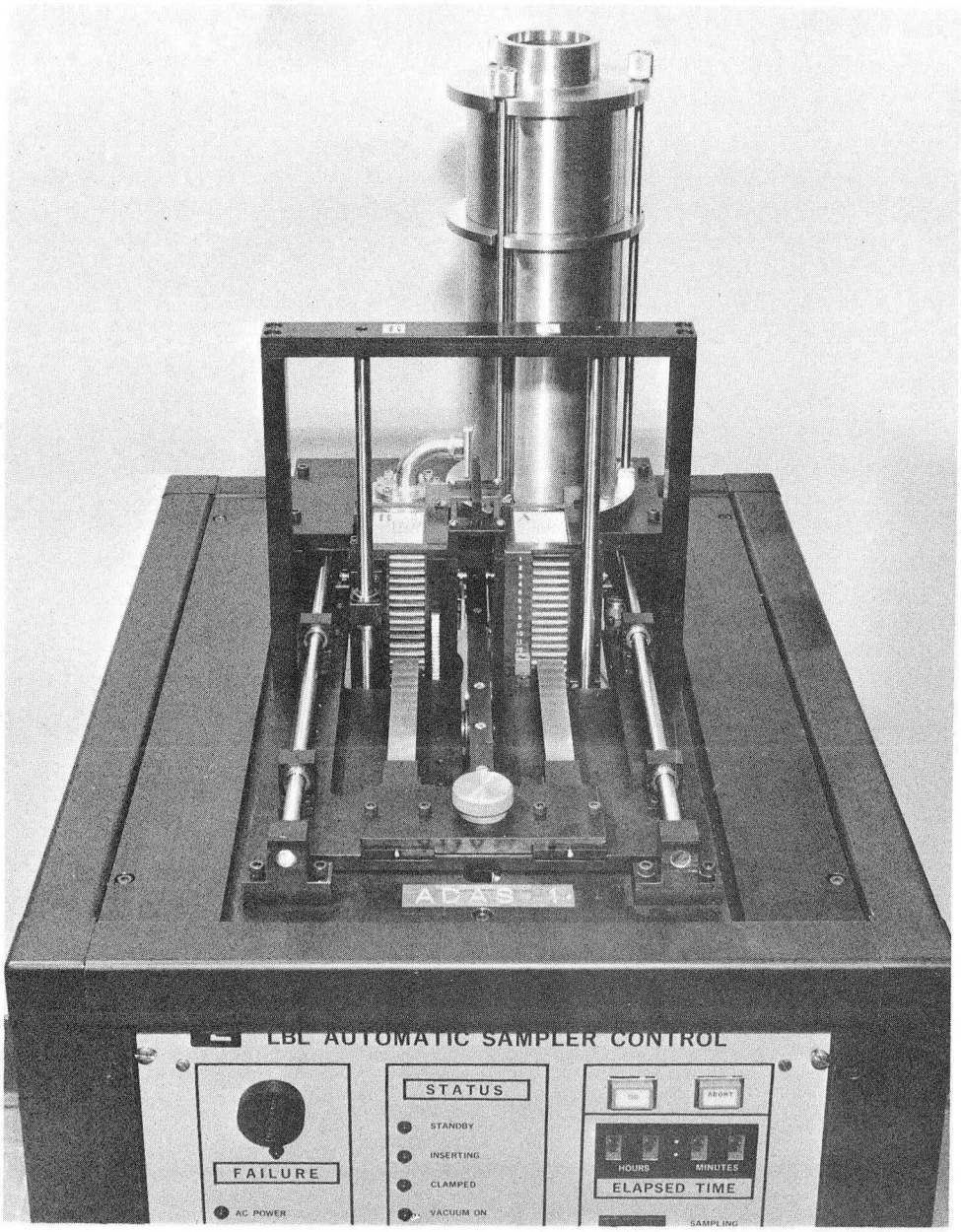

Fig. 22 A close view of the ADAS with dust cover removed.

RESULTS AND DISCUSSION

Thirteen sampling units of the type described have been built. A high degree of uniformity has been achieved particularly on the critical virtual impactor parameters. For example, the spread of the pressure differentials P_1 required to draw 50.1 ℓ/min of air is less than 1% among all the samplers. The difference in cut point between two different units was measured to be less than 0.1 μm.

SIZE SEPARATION AND LOSSES

The results of an evaluation of a typical sampler are summarized in Table 3 and 4 and the overall results are plotted in Fig. 23. Loss measurements are tabulated for specific regions. Region 1 losses include those washed from parts 1 and 2 of Fig. 16, region 2 from parts 3 and 4, region 3 from parts 5 and 6, and regions 4 and 5 are from parts 7 and 9 respectively. There are two obvious components of losses. A loss peak near the size cut point reflects the intrinsic tendency for particles of the cut point size to be intercepted by the physical surface which deflects the streamlines (in this case the inner rim of the receiving tubes). The observed fact that there is no deposition on the top of the tubes suggests that the virtual impaction surface is somewhat below the opening to the tubes. The coarse particles loss component is mostly gravitational settling on the cone (part 6) in the drift tube. In the specific design shown in Fig. 16, impaction losses were found for large particles on part 6. A later modification added 7.6 cm to the length of the drift tube to eliminate this component. The tabulated measurements reflect this modification.

The high sticking probability of the liquid DOP particles to the wall and to each other leads to the exaggerated loss condition. A pronounced reduction in losses is observed for solid uranine particles. The E vs. D_p plot shows a very sharp cut characteristic. Its long term stability (months) enables us to define the aerodynamic size of solid particles whose final density is less well known. The slight down shift of the solid particle loss peak compared with that of the liquid is consistent with the expectation that large solid particles are more likely to bounce.

PARTICLE SIZE (μm)	1.34	1.81	2.21	2.64	3.10	4.11	6.05	8.06	10.04
REGION 1	0	0	0.5	0.8	0	0	0	0.1	0.3
REGION 2	0	0.7	4.1	11.9	11.0	0	0	0	0
REGION 3	0	0	0	0	0.1	0.2	0.5	0.8	1.0
REGION 4	0	0	0.7	0	0	0	0	0	0
REGION 5	0.1	1.9	4.9	10.7	8.0	0.6	0.6	0	0
TOTAL LOSS	0.1	2.6	10.2	23.4	19.1	0.8	0.5	0.9	1.3
FILTER A	6.5	11.9	23.6	6 0.1	79.2	99.1	99.4	99.1	98.7
FILTER B	93.4	85.5	66.4	16.7	1.7	0	0	0	0
E = A/(A + B)	6.5	12.2	26.2	78.3	97.9	100	100	100	100

TABLE 3 Summary of evaluation with liquid DOP particles (Percent deposition of particles on sampler and filters)

PARTICLE SIZE (μm)	1.00	1.61	2.18	2.94	3.50
REGION 1	0	0	0	0	0
REGION 2	0	0	0.1	0.6	0
REGION 3	0	0	0	0	0.1
REGION 4	0	0	0	0	0
REGION 5	0	0	1.3	1.6	0.2
TOTAL LOSS	0	0	2.4	2.2	0.3
FILTER A	4.7	8.7	24.4	93.0	99.6
FILTER B	95.3	91.3	74.2	4.8	0.1

TABLE 4 Summary of evaluation with solid uranine particles (percent deposition of particles on sampler and filters)

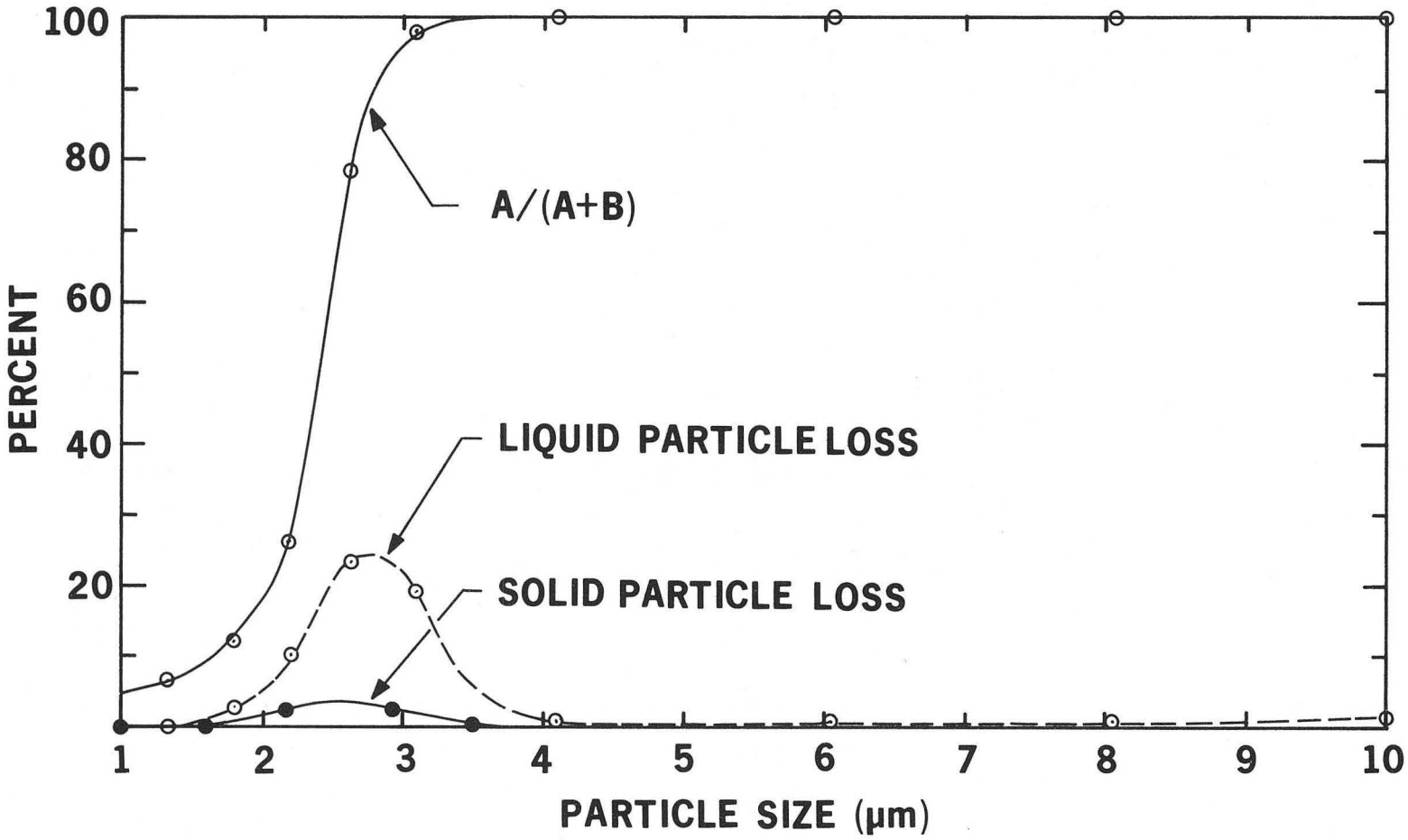

XBL 751-124

Fig. 23 Particle size segregation characteristics and losses as a function of particle size.

FLOW CONTROL

The null switch for the pressure sensor is set to reduce hysteresis errors to less than 0.5%. The repeatability in flow rate is typically better than 0.2%. If constant pressure drop is maintained across a set of fixed orifices, the mass flow, to a first approximation, is inversely proportional to the square root of the absolute temperature. Aerosol concentrations are conventionally expressed in units of mass per unit volume. Thus, the volume flow needed is directly proportional to the square root of the absolute temperature.

As the in-take air is cooled from 20°C to -35°C, the automatic micrometer valve shows little adjustment as long as clean filters are used in the device. When heavily-loaded filters are in place, a slight closing of the micrometer vavle is observed as the temperature is lowered, suggesting the larger viscosity contribution to the pressure drop across the loaded filter.

STABILITY AND RELIABILITY

The flow calibration drift over a three month period was measured to be under 0.5%. The almost continuous sampling over the same period produced no detectable change in the 2.5 ℓ/min limiting orifice behind filter A.

The samplers have been extensively tested under laboratory conditions by continuously recycling filters over an extended period. An equivalent of 15,000 samples have been run as part of this study. After eliminating obvious problems in the initial debugging period, the average failure probability has been reduced to less than 0.1% per sample.

LIMITATIONS

A real instrument often falls short of ideal performance due to compromises made to satisfy practical boundary conditions. The physical size of the apparatus sets an upper limit on the largest particle that may be efficiently sampled. For example, the 10 μm particle loss is less than 1.5% for liquid particles, but there is a sharp rise to 70% at 20 μm caused by impaction on sidewalls and by gravitational settling.

Some of the limitations arise from the properties of the filter medium selected. An ideal filter should exhibit high filtration efficiency, homogeneity, mass loading capability, and mechanical strength, and should exhibit low trace impurity content, flow impedance, mass thickness and moisture uptake, as required by beta gauge and X-ray fluorescence measurements. Some of these requirements are obviously mutually exclusive. The 1.2 μm cellulose membrane filter used is considered a good compromise. The power and weight considerations on the vacuum pump lead to the choice of a pump that will maintain the desired sampling rate of 50 ℓ/min for up to a 70% increase in filter impedance over its nominal value of 26.2 torr-cm^2/ℓ/min. The corresponding loading on the fine particle filter, which bears the main flow, is about 200 μg/cm^2. This leads to the limitation that in heavily polluted air with 100 μg/m^3 of fine particles, the maximum sampling time will be limited to approximately 4.5 hours.

As presently packaged in the sound insulated chamber, the pump requires cooling air at a temperature below 35°C to avoid accelerated wear.

CONCLUSION

Of the thirteen samplers, ten are installed and operating in the St. Louis RAMS network. It has been demonstrated that the virtual impactor, with its distinct advantages over its conventional counterpart, has fulfilled the need for an instrument to collect aerosols in two strategic size ranges. The adaptability of the virtual impactor to automation and its compatibility to other analytical instruments suggests that it may be suited for wider use. Refinements on the range of acceptable particle size, filter impedance and filter mass loading should further improve its potential for large scale deployment.

ACKNOWLEDGEMENTS

The authors wish to express their gratitudes to T. Dzubay of EPA and C. Peterson of ERC for making the ERC virtual impactor available for evaluation. We acknowledge the contributions of the following LBL staff: R. Adachi, O. Arrhenius, C. Cyder, B. Jarrett, N. Madden, J. Meng, H. Riebe, A. Roberts, W. Searles, D. Vanacek and S. Wright. The fabrication of thirteen samplers would not have been

possible without the great support from the personnels of the Electronics and Mechanical Shops.

We also appreciate the cooperation of H. Schneider and R. Leiser of the Nuclepore Corporation in developing cellulose membrane filters of acceptable quality and mounted appropriately. We are indebted to B. Liu of the University of Minnesota for evaluating filter efficiency, and R. Giauque of LBL for analyzing filter impurity content.

REFERENCES

1. Goulding, F. S. and J. M. Jaklevic, Photon-Excited Energy Dispersive X-ray Fluorescence Analysis for Trace Elements. Annual Review of Nuclear Science, 23:45-74, 1973.

2. Goulding, F. S. and J. M. Jaklevic, X-ray Fluorescence Spectrometer for Airborne Particulate Monitoring. Environmental Protection Agency Publication No. EPA-R2-73-182, April 1973.

3. Whitby, K. T., R. B. Husar and B. Y. H. Liu, The Aerosol Size Distribution of Los Agneles Smog. In: Aerosols and Atmospheric Chemistry, Hidy, G. M. (ed.). Academic Press, 1972. p. 237-264.

4. Whitby, K. T., On The Multimodal Nature of Atmospheric Aerosol Size Distribution. Particle Technology Lab Publication No. 218. University of Minnesota, 1973.

5. Air Quality Criteria for Particulate Matter, Chapter 9. National Air Pollution Control Administration Publication No. AP-49, 1969.

6. Conner, W. D., An Inertial-Type Particle Separator for Collecting Large Samples. Journal of the Air Pollution Control Association. Vol. 16, No. 1:35-38, January 1966.

7. Hounam, R. F. and R. J. Sherwood, The Cascade Centripeter: A Device for Determining the Concentration and Size Distribution of Aerosols. American Industrial Hygiene Association Journal. Vol. 26, No. 2:122-131, March-April 1965.

8. Loo, B. W. and J. M. Jaklevic, An Evaluation of the ERC Virtual Impactor. Lawrence Berkeley Laboratory Report No. LBL-2468. January 1974.

9. Marple, V. A., A Fundamental Study of Inertial Impactors. Doctoral Thesis, Department of Mechanical Engineering, University of Minnesota. December 1970.

TECHNICAL INFORMATION DIVISION
LAWRENCE BERKELEY LABORATORY
UNIVERSITY OF CALIFORNIA
BERKELEY, CALIFORNIA 94720